Effect of Torque-Tube Parameters on Rear-Irradiance and Rear-Shading Loss for Bifacial PV Performance on Single-Axis Tracking Systems

Preprint

Silvana Ayala Pelaez,[1] Chris Deline,[1] Joshua S. Stein,[2] Bill Marion,[1] Kevin Anderson,[3] and Matthew Muller[1]

1 National Renewable Energy Laboratory
2 Sandia National Laboratories
3 Cypress Creek Renewables

Presented at the 46th IEEE Photovoltaic Specialists Conference (PVSC 46)
Chicago, Illinois
June 16–21, 2019

NREL is a national laboratory of the U.S. Department of Energy
Office of Energy Efficiency & Renewable Energy
Operated by the Alliance for Sustainable Energy, LLC

This report is available at no cost from the National Renewable Energy Laboratory (NREL) at www.nrel.gov/publications.

Contract No. DE-AC36-08GO28308

Conference Paper
NREL/CP-5K00-73203
October 2019

Effect of Torque-Tube Parameters on Rear-Irradiance and Rear-Shading Loss for Bifacial PV Performance on Single-Axis Tracking Systems

Preprint

Silvana Ayala Pelaez,[1] Chris Deline,[1] Joshua S. Stein,[2] Bill Marion,[1] Kevin Anderson,[3] and Matthew Muller[1]

1 National Renewable Energy Laboratory
2 Sandia National Laboratories
3 Cypress Creek Renewables

Suggested Citation
Ayala Pelaez, Silvana, Chris Deline, Joshua S. Stein, Bill Marion, Kevin Anderson, and Matthew Muller. 2019. Effect of Torque-Tube Parameters on Rear-Irradiance and Rear-Shading Loss for Bifacial PV Performance on Single-Axis Tracking Systems: Preprint. Golden, CO: National Renewable Energy Laboratory. NREL/CP-5K00-73203. https://www.nrel.gov/docs/fy20osti/73203.pdf.

NREL is a national laboratory of the U.S. Department of Energy
Office of Energy Efficiency & Renewable Energy
Operated by the Alliance for Sustainable Energy, LLC

This report is available at no cost from the National Renewable Energy Laboratory (NREL) at www.nrel.gov/publications.

Contract No. DE-AC36-08GO28308

Conference Paper
NREL/CP-5K00-73203
October 2019

National Renewable Energy Laboratory
15013 Denver West Parkway
Golden, CO 80401
303-275-3000 • www.nrel.gov

NOTICE

This work was authored in part by the National Renewable Energy Laboratory, operated by Alliance for Sustainable Energy, LLC, for the U.S. Department of Energy (DOE) under Contract No. DE-AC36-08GO28308. Funding provided by U.S. Department of Energy Office of Energy Efficiency and Renewable Energy Solar Energy Technologies Office. The views expressed herein do not necessarily represent the views of the DOE or the U.S. Government. The U.S. Government retains and the publisher, by accepting the article for publication, acknowledges that the U.S. Government retains a nonexclusive, paid-up, irrevocable, worldwide license to publish or reproduce the published form of this work, or allow others to do so, for U.S. Government purposes.

Cover Photos by Dennis Schroeder: (clockwise, left to right) NREL 51934, NREL 45897, NREL 42160, NREL 45891, NREL 48097, NREL 46526.

Effect of torque-tube parameters on rear-irradiance and rear-shading loss for bifacial PV performance on single-axis tracking systems

Silvana Ayala Pelaez[1], Chris Deline[1], Joshua S. Stein,[2] Bill Marion[1], Kevin Anderson[3], Matthew Muller[1]

[1]National Renewable Energy Laboratory, Golden CO 80401 USA;
[2]Sandia National Laboratories, Albuquerque, NM 87123 USA;
[3]Cypress Creek Renewables, San Francisco CA 94108 USA

***Abstract* — The emergence of cost-competitive bifacial PV modules has raised the question of the additional value of bifacial 1-axis tracking arrays, in particular when considering rear-irradiance losses from the tracker system itself. In this work, the effect of different geometries and materials of torque tubes is evaluated through ray-trace simulations and found to cause rear irradiance shading factors between 2% to 8% for systems without gap between the modules in 2-UP configuration. Inclusion of a gap between the modules can offset the shading factor. Electrical mismatch is also evaluated for the various configurations, and a methodology to apply shading factor and electrical mismatch loss to rear irradiance from the calculated loss in DC power, which averages 1% for the systems explored here, is proposed.**

***Index Terms* — bifacial PV module, single-axis tracking, irradiance, ray-tracing, model, performance, torque tube**

I. Introduction

An increased industry focus on bifacial modules, which collect light from both front and rear side thereby generating more energy, has translated into a predicted market share of 35% worldwide by 2028 [1]. The use of bifacial modules in single-axis-tracking (SAT) systems promises to increase energy yield further and offset increased system cost, in comparison to conventional SAT with monofacial PV modules. Previous work by the authors has shown measured bifacial energy gains of 7%–9% for a 100 kW commercial tracked system in Klamath Falls, Oregon [2]. Bizarri [3] presented results from the La Silla PV plant in Chile, where a 550-kWp SAT bifacial module array demonstrated a 12% increase in performance with respect to standard SAT monofacial technology. Forecasting of the bifacial gain for La Silla was performed by [4], finding good agreement with the use of hybrid view-factor and ray-tracing approaches. Further modeling with view-factor approaches was presented by [5], finding gains between 3-11% for SAT systems. Although these works examine the dependency of bifacial gain on the local geography and climate, they mimic the tracking geometry with a simplified representation of the tracker system, neglecting surrounding rack or structure shading objects. The calculated rear irradiance is therefore over-predicted without this additional shading loss.

The torque tube and tracking structures introduce shading onto the rear of the panel, leading to mismatched irradiance on the cell level which impacts the performance of bifacial systems [6]. The characterization of this effect is not well studied yet, and typically addressed in simulations by a linear reduction in the calculated rear-irradiance to evaluate the impact on annual performance [7], [8]. PVSyst [9], one of the main due-diligence software tools for evaluating PV projects, utilizes a shading factor that directly reduces the yearly-cumulative rear-irradiance calculated at the collectors by this software [10]. This shading factor is proposed to first order as the ratio of the mechanical shading area (torque tubes, junction boxes, and any other objects between the ground and the modules) to the sensitive area of the module. However, for the case of torque tubes the shape, size, material, and system geometry will modify the irradiance and shading pattern on the rear side of the modules, requiring a more detailed analysis to find the correct system optical shading factor.

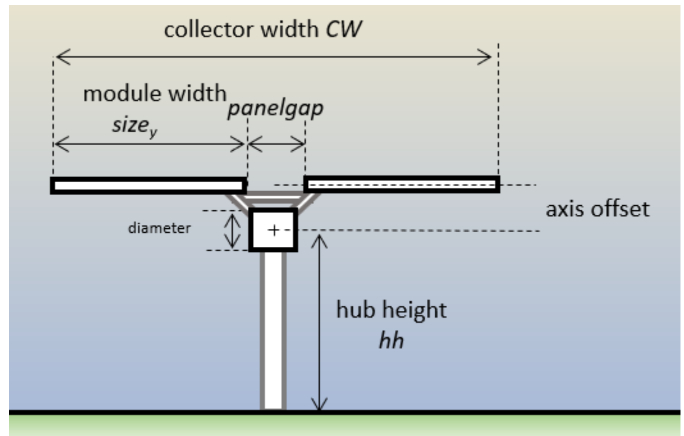

Fig. 1. Single-axis tracker geometry. Panel gap is considered for 2-up systems. Torque tube's centroid is coincident with the rotation axis of the trackers, and panels are offset by a distance *axis offset*.

In this work, we compare field measurements of rear-irradiance of single-axis-tracked bifacial array systems with modeled rear-irradiance profiles based on ray-tracing models that consider tracking and the torque tube's geometries. In prior work, we described a RADIANCE [11] based ray-trace model for rear-side irradiance G_{rear} calculation of fixed and SAT systems, and we verified them with field data [12]–[15]. Here, we extend this model for performing detailed modeling of single-axis-tracking including parametric adjustment of torque-tube parameters.

The Radiance model offers the possibility of reproducing complex scenes, including tracker elements. This model is freely downloadable and can be used to evaluate 1-up and 2-up systems, with various torque tube profiles, diameters, distances between modules, and axis-offsets.

I. Detailed Bifacial Model for SAT

With single-axis tracking, the modules are no longer at a fixed tilt, and the clearances to the ground and with neighboring rows in the array are constantly changing. Tracking algorithms can be used to calculate these parameters based on the ground coverage ratio (GCR):

$$GCR = \frac{CW}{rtr} \quad (1)$$

where *rtr* is the distance between the rotation axis of the panels and *CW* is the width of the modules in a row, defined as:

$$CW = \#_{modules} \times size_y + panelgap \times (\#_{modules} - 1), \quad (2)$$

where *#modules* is the number of modules in the configuration (1 module for 1-up, 2 modules for 2-up, etc.), $size_y$ is the PV module width (independent of the tilt angle), and *panelgap* is the spacing between modules for configurations with more than 1 module along the collector width (Figure 1).

GCR is used in tracking algorithms to implement backtracking corrections to the tilt of the trackers, based on minimizing shading from neighboring arrays. This correction becomes particularly important for arrays with higher GCRs. We can also define a normalized axis height *H*:

$$H = \frac{axis\ height}{CW} \quad (3)$$

These normalized parameters allow comparisons between tracker designs of different dimension (e.g., 2-up landscape vs. 2-up portrait) because the self-shading geometry and bifacial rear irradiance depend on these normalized parameters, not on absolute dimensions. In order to compare systems with different collector widths resulting from varying the panel gaps in this paper, GCR is maintained and rtr is increased accordingly.

It is assumed the torque-tube's centroid coincides with the axis of rotation. The torque tube's profile can vary, and for this paper circular, square, and hexagonal profiles are considered. For hexagonal profiles, the diameter is measured between vertices, corresponding to a circumscribing circle's diameter.

It is assumed that the *axis offset* is larger than or equal to zero. When the axis offset is 0, the modules are co-planar with the torque tube, and the panel gap must be larger than the torque tube's diameter to avoid inconsistencies in the geometry.

Results are presented for a module at the center of a large-scale PV installation to avoid edge-effects in irradiance.

The tracking algorithm from PVLib [16] is used to compute the array tilt throughout the day. Backtracking corrections have been employed to reduce self-shading of the panels at high solar zenith angles based on the GCR of the system. For results presented in this paper, hourly simulations are conducted, either for single days or for each hour in a year. The software also includes an option for cumulative annual simulations reducing computation time by ~200x, but this option was not viable for this applications which requires hourly resolved shade estimation [2].

A. G_{Rear} Shading Factor

To evaluate the impact of the torque tube shadow, an optical shading factor is calculated by averaging rear irradiance over the middle of the center module, either with or without the torque tube:

$$G_{rear}\ Shading\ factor = \frac{\sum_{n=0}^{N} G_{rear}\ (with\ tube)}{\sum_{n=0}^{N} G_{rear}\ (no\ tube)} \quad (4)$$

A typical number of spatial points N used to calculate G_{rear} is one per centimeter of the collector width.

B. G_{Rear} Shading and Electrical Mismatch

The inherent rear-irradiance distribution of a bifacial module can result in an electrical mismatch due to the different irradiances in each cell. Structural shading like the torque tube shadow can modify the rear-irradiance distribution from the cases where no structural shading is considered. This section proposes a methodology for evaluating the impact of electrical mismatch when modeling more complex systems that include structural shading.

Two system are compared to calculate the power loss due to electrical mismatch and shading. The 'baseline' system considers no torque tube shading, and considers the sum of the front and rear average irradiance to calculate the module's power output P_0 :

$$P_0 = \left(G_{F_0} + G_{R_0} \cdot \varphi\right) \cdot \eta_0 \quad (5)$$

where η_0 is the efficiency of the module at the specific irradiance and temperature values, and φ is the bifaciality factor of the bifacial module. $P_0$is compared to $P_1$to calculate the power loss, where $P_1$is the output power of a system that considers the torque tube in the rear irradiance calculation, and further considers nonlinear cell-level mismatch loss. The cell-level irradiance input varied by cell-row according to the detailed profile calculated by the bifacial_radiance software for every hour in the year. The loss in power DC can then calculated such that:

$$L_{DC} = 1 - \frac{P_1}{P_0}. \quad (6)$$

Using the L_{DC} term, P_1 can be expressed with respect to the front and rear average irradiance values of P_0 such that:

$$P_1 = \left(G_{F_0} + G_{R_0} \cdot \varphi\right) \cdot \eta_0 \cdot (1 - L_{DC}) \quad (7)$$

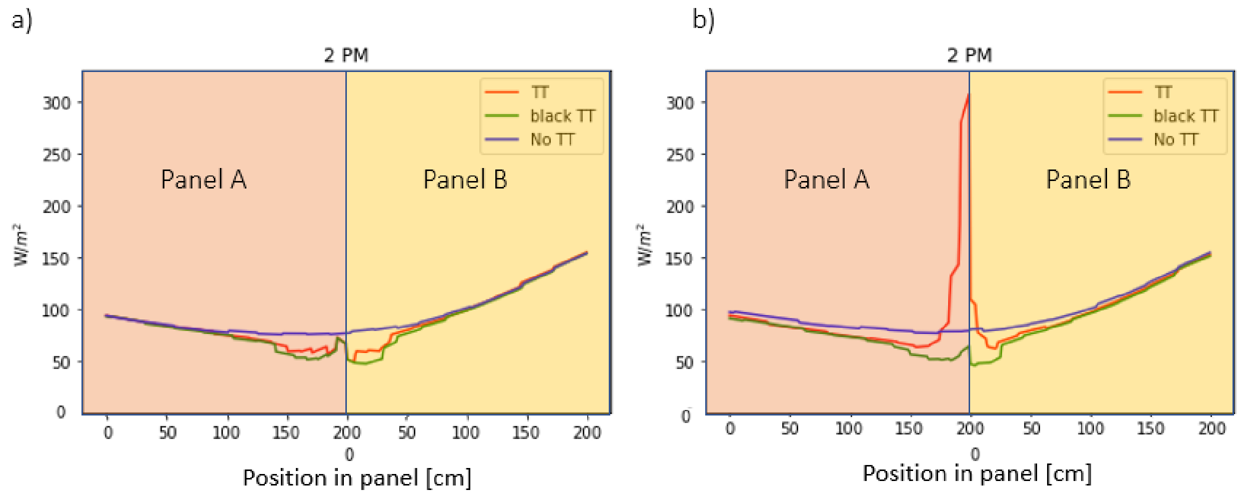

Fig. 2. Rear irradiance profiles for a 2-up system of size = 2m, with a) no gap, and b) a gap of 0.15 m. Gap itself is not plotted, only irradiance in the modules. The blue curve shows the rear irradiance when no torque tube is included, and the green and red torque tube are when a black (absorbing) torque tube and a metal (reflective) torque tube of 0.15 m is considered. Axis offset is 0.75x torque tube diameter.

Current due diligence software that model bifacial systems, like PVSyst and SAM, address rear-irradiance shading and electrical mismatch losses by applying loss coefficients directly to the rear-irradiance (rather than at the system L_{DC} level):

$$P_1 = \left(G_{F_0} + (1 - X)G_{R_0} \cdot \varphi\right) \cdot \eta_0 \tag{8}$$

where the loss factor X represents the inherent electrical mismatch loss and the structural shading loss (i.e. from the torque tube) applied only to G_{rear}:

$$X = L_{Inherent\ Mismatch} + L_{Structural\ Shading} \tag{9}$$

The above equations can be used to solve for X in term of the bifacial gain in irradiance of the system:

$$BG_G = \frac{G_{R_0} \cdot \varphi}{G_{F_0}} \tag{10}$$

$$X = \frac{L_{DC}}{BG_G} + L_{DC} \tag{11}$$

As an example, for a system with a bifacial gain of 10% and system shading and mismatch loss of L_{dc} = 1%, the equivalent rear irradiance loss would be X = 11%.

II. Simulation Results

Rear irradiances were calculated for a 2-UP portrait system with and without torque tube for the location of Richmond, VA. Module size was 1.7 m. Square torque tubes of 0.15m by side were modeled, with either metallic grey (45% reflective), or black (100% absorptive) properties. A GCR of 0.33 and an H of 1.2 were considered. The panel gap between both modules was varied. Figure 2 shows the rear-irradiance distribution for this system with a) no gap (gap = 0) and b) a gap of 0.15m. Shading loss for the no-gap example is 8.1% and 5% for the black and metallic torque tubes. For the case with the gap between modules, reflected light from the torque tube creates regions of increased irradiance near the inner borders of the modules. Optical shading loss (Eq. 4) for black and metal torque tubes are 12% and 0.01% because of this increased irradiance. The profile of the torque tube and sensitivity to the tracking angle accuracy must also be explored, as deviations might move the location of this high-irradiance area in the module creating hot-spots (Figure 3).

In Figure 4, hourly shading factor are averaged over one sunny and one cloudy day for black, square torque tubes. Black torque tubes do not reflect light going through the gap of the 2 modules in the 2-up configuration. For cloudy days, the Grear shading factor is constant at 8.3%. The shading factor for this configuration as defined by PVSyst would be 7.5%. For the clear-sky day, the shading loss increases with the gap size, since the black torquetube absorbs light that would otherwise be reflected to the rear of the modules.

Full year simulations were also run with an hourly resolution for a 2-UP portrait system with and without torque tube for the location of Cairo, Egypt. Twenty modules and seven rows were simulated, with rear irradiances obtained along the center

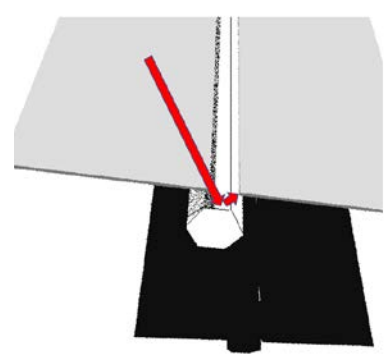

Fig. 3. Reflected direct and diffuse light on the torque tube will create areas of higher irradiance in the rear side of the panel.

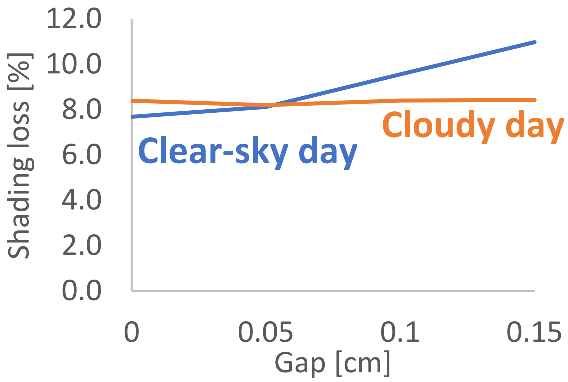

Fig. 4. Shading loss for a clear-sky and a cloudy day, for a single-axis tracking bifacial system with black absorbing torque-tube.

module of the array. Module size was 1x1.5 m in landscape, and the tracker's hub height was set to 2 m, coincident with the axis of rotation of the system. Metallic torque tubes (44% reflective) of 0.1 m in diameter were modeled. Table 1 shows the parameters varied in the simulations, with the baseline parameters marked with an asterisk.

TABLE I. VARIABLES AND VALUES EXPLORED FOR CAIRO YEARLY SIMULATIONS

Variable	*Values*
X-gap [cm]	1*, 5, 10, 25
Z-gap [cm]	5*, 10, 15, 20
Y-gap [cm]	0*, 5, 10, 15, 30
Shape Test:	round*, square, hexagonal, octagonal

* baseline value

A constant *GCR* of 0.28 was assumed for the Cairo simulations, which varied the pitch between the 7 rows accordingly to the collector width for the cases where the spacing between the panels (y-gap) was greater than 0.

Results for the various simulations (Table 2) showed a reduction in shading factor with greater z-gap, with increased z-gap reducing the shading factor to 2% from 6%. This reduction in shading factor resulted in higher bifacial gains for these setups, shown in Table 2. Different torque tube shapes also caused varied the shading factor, in the range of 5%- 7.5%, although no particular trend was evident.

Just as with the daily simulations conducted for Richmond, including a y-gap and reflective torque tube increases the rear-irradiance in the annual simulations for Cairo. Some of the shading factors calculated for the year were negative, implying a gain in the rear irradiance with respect to the baseline case. To evaluate the impact on power-loss of the inherent self-shading of the module and nearby rows and of the shading created by the torque tubes, the electrical performance of the bifacial modules was modeled using PVMismatch [1]. The shading factors and associated loss term X can be seen in Figure 5. On average, L_{DC} was around 1%.

TABLE II. SHADING FACTOR RESULTS.

	Value modified from baseline	Bifacial Gain	Shading Factor
BASELINE NO TUBE	--	14.3	0
BASELINE WITH TUBE	--	13.4	5.7
Shape test	square	13.2	7.5
Shape test	octagon	13.4	6.1
Shape test	hexagon	13.5	5.5
Xgap test	0.05	13.6	4.3
Xgap test	0.1	13.9	2.1
Xgap test	0.25	14.7	-3.6
Zgap test	0.1	13.6	4.6
Zgap test	0.15	13.8	3.4
Zgap test	0.2	13.9	2.3
Ygap test	0.05	14.3	-0.1
Ygap test	0.1	14.5	-1.7
Ygap test	0.15	14.2	0.8
Ygap test	0.3	14.2	1.8

Further research is required to evaluate this and other configurations in different locations to see if these loss factors are generally applicable.

III. SENSOR LOCATION FOR FIELD BIFACIAL SYSTEMS

A bifacial tracked system located in Jackson, Michigan, was investigated for this study to evaluate the placement of rear-irradiance sensors in bifacial systems and provide further validation for the bifacial_radiance ray-trace software. The

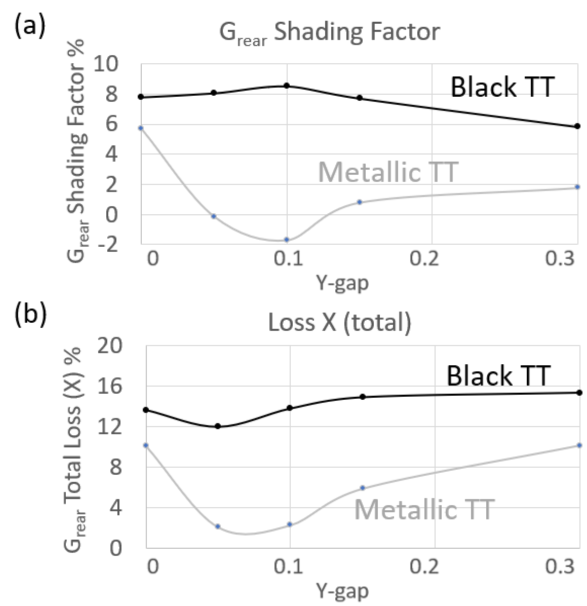

Fig. 5. (a) G_{Rear} shading factor for a 2-up landscape system with varying distances between the modules (Y-gap). Both black (0% reflective) and metallic (44% reflective) torque tubes are evaluated. (b) Loss factor X that should be applied to the rear-irradiance calculation of the 2-UP system to account for the shading and electrical mismatch losses for the different Y-gaps and torque tubes configurations.

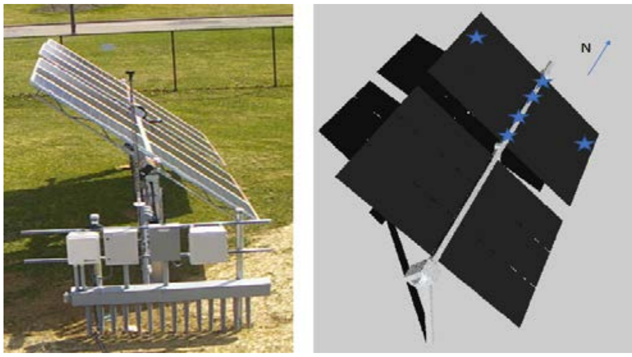

Fig. 6. A photograph (left) and RADIANCE image (right) showing the Jackson, MI single-axis tracked system . Six IMT sensors are mounted on the back of the modules and torquetube to measure rear irradiance.

system consists of a single row of 6 pairs of monofacial panels (on the N and S edges) and bifacial panels, in 2-up configuration. Six IMT reference cells are located as marked in Figure 6. The tracker's hub height is 2.25m, and the albedo for the site was measured for all time-points analyzed on site with two SR05 pyranometers in albedometer orientation. The panels are flush with the torque-tube for this particular modeled geometry, meaning the torque tube is not directly blocking the rear of any of the bifacial modules.

The measured and modeled values for the 6 irradiance sensors are plotted in Figure 7. The model tended to over-estimate measured values by 4%-15%. However, average modeled values fell within the range of minimum and maximum measurements. Mean bias deviation (MBD), and

TABLE III. MBD AND RMSE FOR THE SIX SENSORS MODELED

	MBD %	*RMSE* %	*MBD_abs* [w/m2]	*RMSE_abs* [w/m2]
S1 (north most)	14.2	39.4	6.8	18.9
S2	13.4	38.8	6.4	18.5
S3	17.4	45.7	7.9	20.8
S4 (South-most)	13.3	39.3	6.3	18.5
S5 (West)	4.3	34.3	2.6	20.2
S6 (East)	4.2	36.8	2.5	21.4

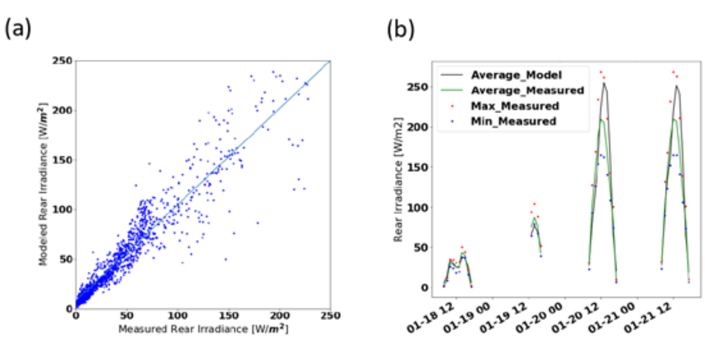

Fig. 7. (a) Measured vs. modeled values for one of the sensors. (b) Example of measured and modeled values for two cloudy and two sunny days. Maximum and minimum measured values are also plotted.

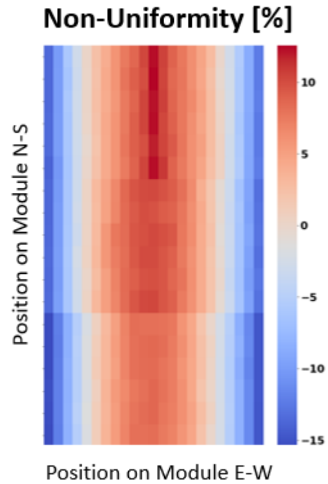

Fig. 8. Non-uniformity mapping of modeled irradiance values at each point compared against the average irradiance across the system. Non-uniformity provides an idea of the modeled variability around the different points.

root mean square error (RMSE) can be seen in Table 3 expressed either as a percent of reading or as absolute Wm^{-2} for the 5 months measurement period, from December to April.

The rear irradiance spatial distribution of the northern half of the tracker system was modeled for a full day, normalized by average irradiance over the system (Figure 8). For this system, modeled rear-irradiance approaches the system average value at a point 20% in from either edge. Edges and middle of the array vary the greatest from the overall average irradiance, which may over- or under-represent G_{rear} averages if a single sensor is used to characterize a bifacial module's back-side average.

IV. SUMMARY

G_{rear} shading factors were calculated for various single-axis tracked bifacial systems, considering simulated hourly irradiance-profiles for a full year. For the modeled systems, shading factors ranged between 2-8%. Some geometries can provide reductions of the shading factors, which can equal potential energy gains. For this same systems, calculated mismatch loss in DC power between systems considering torque tube and systems not considering torque tube and using simplified average rear-irradiance values are between 1%. The ray-trace tool and methodology presented can be used to obtain a more accurate estimation for large-scale bifacial PV installation yields and the energy loss resulting from the tracker configuration. An estimation of the non-uniformity between the rear-irradiance distribution and the average rear-irradiance value of various modules in a single-row was also performed, finding that G_{rear} irradiances deviate the most from the average values near the edges and middle of the collector width.

Acknowledgement

This work was authored [in part] by the National Renewable Energy Laboratory, operated by Alliance for Sustainable Energy, LLC, for the U.S. Department of Energy (DOE) under Contract No. DE-AC36-08GO28308. Funding provided by the U.S. Department of Energy's Office of Energy Efficiency and Renewable Energy (EERE) under Solar Energy Technologies Office (SETO) Agreement Number 30286, 34910 and Award Number DE-EE0008564. [A portion of] The research was performed using computational resources sponsored by the DOE's Office of Energy Efficiency and Renewable Energy and located at the National Renewable Energy Laboratory. The views expressed in the article do not necessarily represent the views of the DOE or the U.S. Government. The U.S. Government retains and the publisher, by accepting the article for publication, acknowledges that the U.S. Government retains a nonexclusive, paid-up, irrevocable, worldwide license to publish or reproduce the published form of this work, or allow others to do so, for U.S. Government purposes.

References

[1] "International Technology Roadmap for Photovoltaic (ITRPV) Results 2017 including maturity report 2018, Ninth Edition, September 2018," 2018.

[2] S. Ayala Pelaez, C. Deline, P. Greenberg, J. S. Stein, and R. K. Kostuk, "Model and Validation of Single-Axis Tracking with Bifacial PV - Preprint," *Golden Co Natl. Renew. Energy Lab. NREL/CP-5K00-72039.*, no. October, 2018.

[3] F. Bizarri, "Innovative bifacial pv plant at la Silla Observatory in Chile," in *4th Bifi PV Workshop, Konstanz, Germany*, 2017.

[4] D. Berrian, J. Libal, M. Klenk, H. Nussbaumer, and R. Kopecek, "Performance of Bifacial PV Arrays with Fixed Tilt and Horizontal Single Axis Tracking: Comparison of Simulated and Measured Data," in *7th World Conference on Photovoltaic Energy Conversion (WCPEC-7). Waikoloa, HI.*, 2018, pp. 1–6.

[5] M. Chiodetti, A. Lindsay, P. Dupeyrat, D. Binesti, E. Lutun, K. Radouane, S. Mousel, "PV Bifacial Yield Simulation with a Variable Albedo Model," in *32nd European Photovoltaic Solar Energy Conference and Exhibition*, 2016, pp. 1449–1455.

[6] C. Caufield, J. Guerrero, and NREL, "Large single-axis trackers for bifacial systems Soltec," *Bifacial PV Workshop*, no. September. 2018.

[7] J. Meydbray, "Barriers to Financing Bifacial PV Projects," *Present. 5th Bifi PV Work. Denver, Color.*, pp. 1–15, 2018.

[8] R. Bailey and J. Jaubert, "A Simplified Method To Approximate Bifacial System Mismatch Losses," in *presented at the 5th Bifi PV Workshop, Denver, Colorado*, 2018, no. August.

[9] A. Mermoud and B. Wittmer, *Pvsyst User's Manual*. PVSyst SA, 2014.

[10] A. Mermoud and B. Wittmer, "Bifacial shed simulation with PVSyst," *4th Bifi PV Work. Konstanz, Ger.*, 2017.

[11] G. Ward, J, "The RADIANCE Lighting Simulation and Rendering System," in *21st Annual Conference on Computer Graphics and Interactive Techniques*, 1994, pp. 459–472.

[12] S. Ayala Pelaez, C. Deline, S. Macalpine, B. Marion, J. S. Stein, and R. K. Kostuk, "Comparison of bifacial solar irradiance model predictions with field validation," *IEEE J. Photovoltaics*, vol. 9, no. 1, pp. 82–88, 2019.

[13] B. Marion, S. MacAlpine, C. Deline, A. Asgharzadeh, F. Toor, D. Riley, J. S. Stein, and C. Hansen, "A Practical Irradiance Model for Bifacial PV Modules: Preprint," in *44th IEEE Photovoltaic Specialists Conference. Washington, DC.*, 2017.

[14] C. Deline, S. MacAlpine, B. Marion, F. Toor, A. Asgharzadeh, and J. S. Stein, "Assessment of Bifacial Photovoltaic Module Power Rating Methodologies—Inside and Out," *IEEE J. Photovoltaics*, vol. 7, no. 2, pp. 575–580, 2017.

[15] S. Ayala Pelaez, C. Deline, P. Greenberg, J. S. Stein, and R. K. Kostuk, "Model and Validation of Single-Axis Tracking With Bifacial PV," *IEEE J. Photovoltaics*, vol. 9, no. 3, pp. 715–721, 2019.

[16] W. F. Holmgren, R. W. Andrews, A. T. Lorenzo, and J. S. Stein, "PVLIB python 2015," in *2015 IEEE 42nd Photovoltaic Specialist Conference (PVSC)*, 2015, pp. 1–5.